

Computation of Choked and Supersonic Turbomachinery Flows by a Modified Potential Method

W. G. Habashi*

Concordia University, Montreal, Quebec, Canada

M. M. Hafez*

Computer Dynamics Inc., Virginia Beach, Virginia

and

P. L. Kotiuga†

Pratt & Whitney Canada Inc., Longueuil, Quebec, Canada

The classical potential formulation is shown to produce nonunique solutions in choked internal flow calculations. A new model is presented with which a potential solution of a choked, or unchoked internal flow with a prescribed back pressure can be obtained. The approach is extended to turbomachines and is capable of solving the unique incidence problem of supersonic inlet cascades. The model includes an essential correction to the potential accounting for nonisentropic shocks. As a second and more accurate approach it is proposed to simplify the Euler equations by using a stream function formulation. The flow downstream of the shock is considered rotational and the vorticity distribution calculated in terms of the entropy gradient behind the shock via Crocco's relation. In both approaches the shock position is adjusted such that the proper entropy rise is produced and, hence, the prescribed back pressure attained. Numerical results, based on an artificial compressibility finite element implementation of the two methods, are presented.

Nomenclature

A	= cross-sectional area of nozzle
$e^{-\Delta S/\bar{R}}$	= entropy function across a shock
M	= Mach number
m	= meridional direction in a cascade
\dot{m}	= mass-flow rate
p	= pressure
q	= velocity $\sqrt{u^2 + v^2}$
r	= radial direction in a cascade
R	= residual of governing partial differential equation
\bar{R}	= universal gas constant
S	= entropy
u, v	= x and y velocity components
x, y	= Cartesian coordinates
β	= flow angle with respect to x -axis
γ	= isentropic exponent
ρ	= density
$\bar{\rho}$	= artificial compressibility
Ψ	= stream function
ϕ	= perturbation potential
Φ	= full potential
θ	= tangential direction in a cascade
ω	= vorticity
Δ	= change in a quantity

Subscripts

B	= back (for imposed back pressure)
$e, e-1$	= element, preceding element in streamline direction
E	= exit
i	= nodal index
I	= inlet
$L-2$	= residual (ΣR_i^2)
n	= normal

s	= shock
S	= static
o	= stagnation
∞	= freestream value

Superscript

$()'$	= ideal or isentropic value
--------	-----------------------------

Introduction

AN accurate simulation of inviscid transonic and supersonic flows is needed in internal and turbomachinery flow problems. The classical potential formulation is proving inadequate and, as will be demonstrated, inapplicable to internal flows because it does not account for losses across shocks.

The assumption that the flow is everywhere isentropic and irrotational limits the range of applicability of the potential model since then only the mass and energy are conserved across a shock but not momentum—the normal momentum losses representing the drag in this case. In the exact inviscid model, however, all three quantities are conserved (Rankine-Hugoniot relations) and the drag is then related to the entropy rise across a shock.

In addition, although for many external flows the potential solution may be considered a good approximation to the Euler one, a potential solution may not exist at all in internal flows with a prescribed back pressure. When it exists, then the shock position is not unique. In fact, it is the entropy rise in the Euler system of equations that determines the shock location.

As a first approximation to the Euler solution of internal flows, we propose to use the potential approach but modify the density and pressure behind the shock by the entropy function, while neglecting the vorticity downstream of the shock especially if the latter's curvature is small.

This approach should work well if the shock extends across the channel but may lead to some difficulties if the shock terminates in the field. In this instance the entropy jump cannot be assumed uniform but must be considered variable, with an associated vorticity distribution. Hence, an alternate and more appropriate approach, where both the entropy

Presented as Paper 83-404 at the AIAA/SAE/ASME 19th Joint Propulsion Conference, Seattle, Wash., June 27-29, 1983; received July 12, 1983; revision received April 13, 1984. Copyright © by W. G. Habashi. Published by the American Institute of Aeronautics and Astronautics, Inc., with permission.

*Consultant, Pratt & Whitney Canada Inc. Member AIAA.

†Aerodynamics Engineer.

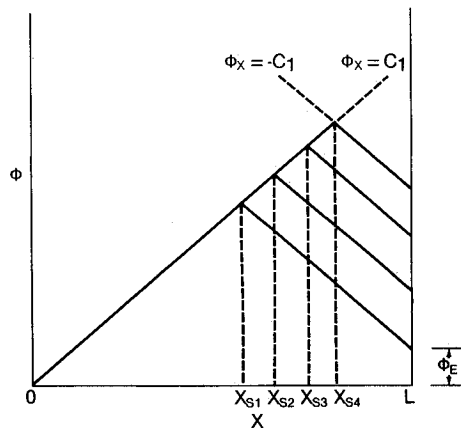


Fig. 1 Nonuniqueness of shock position in a nozzle for Neumann exit boundary conditions.

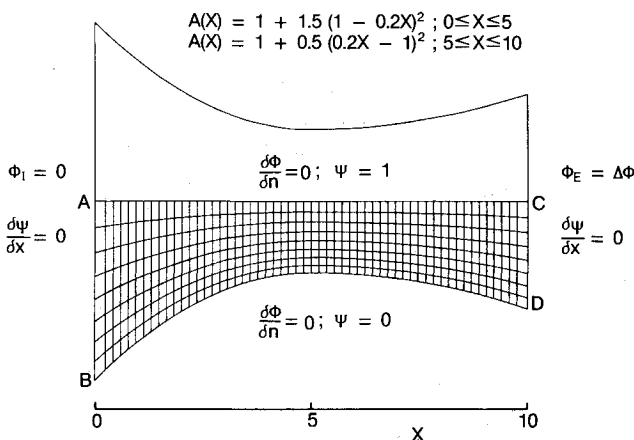


Fig. 2 Profile and grid for nozzle; grid: (57 × 9) bilinear quadrilateral finite elements.

variation and the corresponding vorticity are easily accounted for, is the stream function formulation. Downstream of a shock the vorticity is proportional to the pressure along streamlines and hence can be easily calculated everywhere.

In this paper both aforementioned approaches are examined. A test problem is presented for the flow over an airfoil in a wind tunnel with a subsonic inlet condition using both methods and for the choked flow through a convergent-divergent nozzle using the modified potential approach. The unique incidence problem associated with supersonic inlet conditions in planar or annular cascades is also resolved using the new modified potential formulation.

All results are obtained using bilinear four node finite elements and the artificial compressibility method.¹ The resulting algebraic equations are solved iteratively by a variety of methods detailed in Ref. 2. The numerical results are compared to the corresponding Euler solutions and the advantages of the present approach are discussed.

Boundary Conditions for Choked Flows

Consider, as an example, the one-dimensional small disturbance model equation

$$(\phi_x^2)_x = 0 \quad (1)$$

in the domain $x=0$ to $x=L$. The upstream boundary conditions for a supersonic flow are

$$\phi(0) = 0; \quad \phi_x(0) = C_1 \quad (2)$$

In order to simulate the presence of a shock a subsonic downstream boundary condition must be specified. Two alterna-

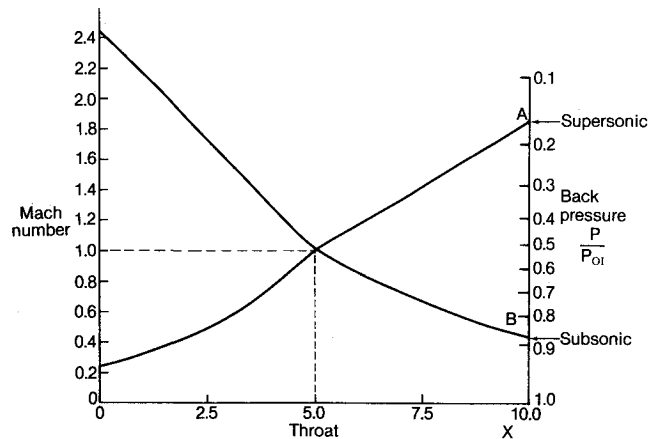


Fig. 3 Isentropic quasi-one-dimensional solution envelopes for nozzle of Fig. 2.

tives are possible

$$\phi_x(L) = C_2 \quad (3a)$$

or

$$\phi(L) = C_3 \quad (3b)$$

The integration of Eq. (1) is

$$\phi_x^2 = C_4^2 \text{ i.e., } \phi_x = \pm C_4 \quad (4)$$

From Eq. (2), $C_4 = C_1$ and from Eq. (3a), $C_2 = -C_4 = -C_1$. Figure 1 illustrates how the shock position X_s cannot be uniquely determined for this exit boundary condition. However, with $\phi(L)$ prescribed, as in Eq. (3b), X_s can be uniquely determined as

$$X_s = L - [\phi(X_s) - C_3] / C_1 \quad (5)$$

Hence, by varying the values of ϕ at $X=L$, the shock position will vary accordingly. Deconinck and Hirsch³ suggest this procedure for nozzle problems assuming the exit flow is parallel in the two-dimensional case, i.e., $v = \phi_y = 0$, hence, $\phi(L)$ is a constant. We use the same nozzle (Fig. 2) presented in that reference to illustrate our approach.

Modified Potential for Quasi-One-Dimensional Choked Nozzle Flows

The governing equation for compressible flow in a nozzle with a cross section $A(x)$ is

$$\rho u A = \text{const} \quad (6)$$

where $\rho = \rho(u)$. This equation can be solved analytically to produce $u = u(x)$ giving two isentropic solutions, with a saddle point at the sonic line, and these are illustrated for the present nozzle in Fig. 3.

The possible flows in the nozzle will now be discussed. For subsonic inlet conditions the flow will expand to the throat followed by compression in the divergent part of the nozzle (branch B). If the flow reaches sonic conditions at the throat, however, it may continue expanding to supersonic flow (branch A) in the divergent part of the nozzle and a shock can be formed by jumping from the supersonic to the subsonic branch (B) [Fig. 4].

Similarly, starting from supersonic inlet conditions the flow will compress to the sonic condition at the throat and, depending on back pressure, may expand in the divergent part of the nozzle following the supersonic branch (A) or may continue to compress following the subsonic branch (B). There is, however, a possibility for the flow to jump from the supersonic branch (A) to the subsonic branch (B) through a shock. In both cases (Fig. 4) the position of the shock can only

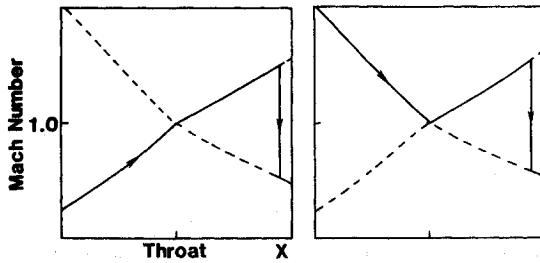


Fig. 4 Two possible nozzle operating conditions producing the same entropy jump.

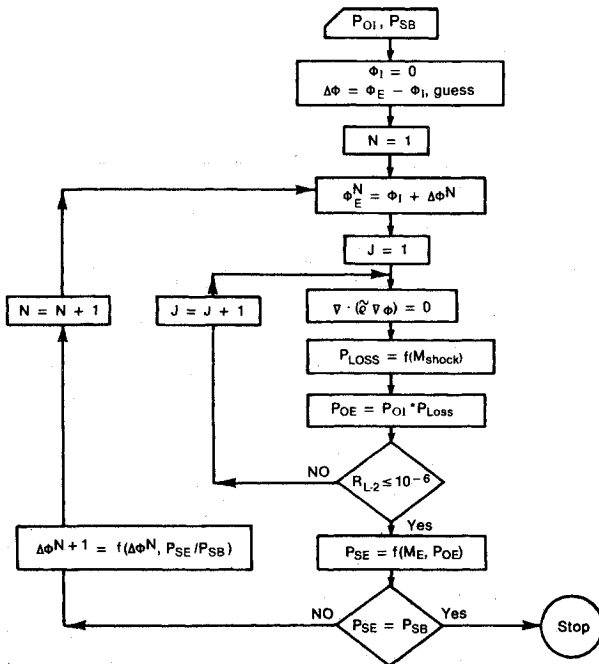


Fig. 5 Iterative scheme for determining shock position for an internal flow with a specified back pressure by the modified potential method.

be uniquely determined by accounting for the entropy jump to match the back pressure. (In this work only compression shocks in the divergent part of the nozzle are considered.)

Let us now introduce a velocity potential, Φ , in Eq. (6). Furthermore, let us replace ρ by $\bar{\rho}$, an artificial compressibility¹ to produce the numerical dissipation necessary for the stability of supersonic flow calculations and to capture shocks, if any exist. Equation (6) then becomes

$$(\bar{\rho} \Phi_x A)_x = 0 \quad (7a)$$

$$\bar{\rho} = \rho - \mu(\rho_e - \rho_{e-1}); \quad \mu = \max[0, 1 - 1/M_e^2, 1 - 1/M_{e-1}^2] \quad (7b)$$

With Φ prescribed at the exit, a discontinuous solution can be obtained with a shock in the divergent part of the nozzle. If the flow is assumed isentropic and if the back pressure is specified between the subsonic and supersonic isentropic conditions, the classical potential solution does not exist. To achieve a prescribed back pressure, the shock loss must be considered. Since this loss (entropy rise) is a function of the Mach number upstream of the shock, the shock position is thus uniquely determined.

The following iterative scheme can then be used in the quasi-one-dimensional case and is detailed in Fig. 5. In the inner loop assume a certain value of Φ_E at the nozzle exit ($\Phi_I = 0$) and solve the problem until a shock appears. The entropy generated across the shock is calculated and used to

modify the stagnation density and total pressure after the shock

$$\frac{\Delta S}{\bar{R}} = \ln \left\{ \left[\frac{2\gamma M_s^2}{\gamma+1} - \frac{\gamma-1}{\gamma+1} \right]^{1/(\gamma-1)} \left[\frac{\frac{\gamma+1}{2} M_s^2}{1 + \frac{\gamma-1}{2} M_s^2} \right]^{\gamma/(\gamma-1)} \right\} \quad (8a)$$

$$p = (\rho' \gamma / \gamma M_\infty^2) e^{-\Delta S/\bar{R}}; \quad \rho = \rho' e^{-\Delta S/\bar{R}} \quad (8b)$$

$$\rho' = \left[1 - \frac{\gamma-1}{2} M_\infty^2 (q^2 - 1) \right]^{1/(\gamma-1)} \quad (8c)$$

After a certain residual convergence criterion is attained (here, $R_{L-2} = 10^{-6}$) the calculated exit pressure (p_{SE}) is verified against the desired back pressure (p_{SB}) and they will not, in general, be equal. The shock position is affected by modifying the value of Φ_E and the loop repeated until the calculated associated back pressure matches the desired one.

It should be noted that for this one-dimensional flow the velocity u can still be replaced by a potential gradient Φ_x without any loss of generality since there is no vorticity. The density, however, has to be modified by a jump in entropy.

Two-Dimensional Choked Nozzle Flows

Considering two-dimensional effects, the transonic problem can be solved numerically using the two-dimensional potential equation, with artificial compressibility

$$(\bar{\rho} \Phi_x)_x + (\bar{\rho} \Phi_y)_y = 0 \quad (9)$$

and the associated boundary condition at the walls or axis of symmetry

$$\bar{\rho} \Phi_n = 0 \quad (10)$$

Similar to the one-dimensional case the values of Φ_I at the inlet and Φ_E at the exit may be specified. Changing $\Delta\Phi$ (i.e., $\Phi_E - \Phi_I$) changes the shock position. Again, there are two isentropic solutions; the subsonic branch and the supersonic branch and, if the exit static pressure is prescribed in between, the classical isentropic potential solution does not exist. Taking into consideration the jump in entropy across the shock, the flow downstream of the discontinuity is of different entropy level and is rotational if the shock is curved. Since shock curvature is small in a nozzle, and the shock extends from one wall to another, a simplified model where the entropy is assumed uniform downstream of the shock may suffice. Hence, the flow is considered isentropic and irrotational (i.e., potential) both upstream and downstream of the shock with, however, a jump in the entropy level. The iterative procedure used in this instance is similar to the one-dimensional case discussed previously and detailed in Fig. 5.

Numerical results are shown in Fig. 6 for a back pressure value of 12.41 psia for the nozzle of Fig. 2. Results excluding and including entropy are shown and compared against the one-dimensional exact solution. The potential, modified by the entropy jump, matches the exact solution well.

In our solution, for a given $\Delta\Phi$, unlike Ref. 3, we account for the entropy rise across the shock during the iteration proper and, hence, we affect the shock position and the flow speed behind it. Furthermore, the monitoring of the back pressure is direct rather than by using an interpreted static pressure depending on the shock loss as in Ref. 3.

A better approximation still would be to consider the effects of variation of the entropy from one streamline to another. This would be needed, in particular, if the shock terminates in the field to prevent a discontinuity in the en-

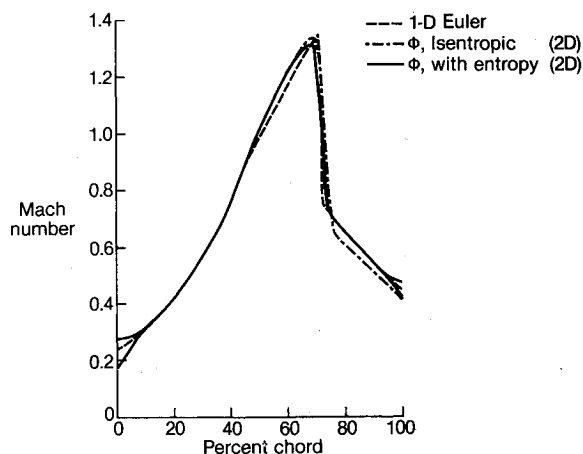


Fig. 6 Two-dimensional, classical, and modified potential solutions for the convergent-divergent nozzle and comparison to exact one-dimensional solution, back pressure 12.41 psia, (57×9) grid, 448 bilinear quadrilateral elements, $\Delta\Phi = 594$.

entropy function where the shock vanishes from creating a problem. Although, strictly speaking, vorticity is generated when entropy varies across the streamlines, it is assumed that it has a negligible effect on the velocity field.

Finally, it should be pointed out that, in Ref. 4, the modified potential formulation had been given in terms of a variational principle where the potential minimizes the integral of the pressure including the entropy effect, namely,

$$I = - \iint p dA \quad (11)$$

where

$$p = (\rho' \gamma / \gamma M_\infty^2) e^{-\Delta S/R}$$

and

$$\rho' = \left[1 - \frac{\gamma-1}{2} M_\infty^2 (q^2 - 1) \right]^{1/(\gamma-1)}$$

In the section entitled Stream Function Formulation, both entropy and the associated vorticity will be included using a stream function formulation.

Supersonic Cascades and the Unique Incidence Problem

To increase mass-flow rate and pressure ratio in a compressor, supersonic Mach numbers at the inlet are utilized. Providing that the axial component of the incoming flow is subsonic a supersonic cascade will operate, for each inlet Mach number, at a single inlet angle. This phenomenon, which has been verified both theoretically and experimentally is known as the unique incidence.^{5,6} Essentially, for supersonic incoming flow, waves of either expansion or compression type will emanate from the suction side of the leading edge of a blade in a staggered cascade as the flow tries to negotiate this convex or concave profile. Since the axial Mach number is subsonic, these waves propagate ahead of the leading edge of the adjacent blade, affecting the flow incidence of this blade. The phenomenon gets repeated and because of the periodicity of flow in a cascade, a unique angle of incidence, as well as a unique inlet Mach number, at all blades, must result. Furthermore, if the leading edge shock gets swallowed in the cascade, due to a lowering of back pressure, then the inlet Mach number and its angle of incidence to the blade remain insensitive to a further lowering of the back pressure. Thus, in a supersonic cascade, neither the inlet Mach number nor the inlet flow angle can be imposed a priori but must be found as part of the solution.

It is also recognized that the appropriate exit boundary condition in a cascade is the specification of a back pressure (i.e., a pressure ratio) which, in general, will be lower than the

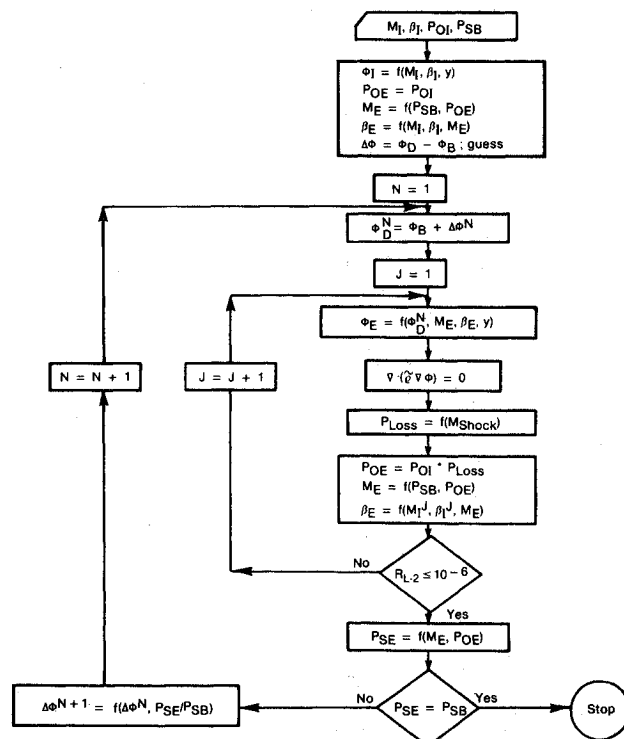


Fig. 7 Iterative procedure for determining potential solution for a supersonic inlet Mach number in a staggered cascade.

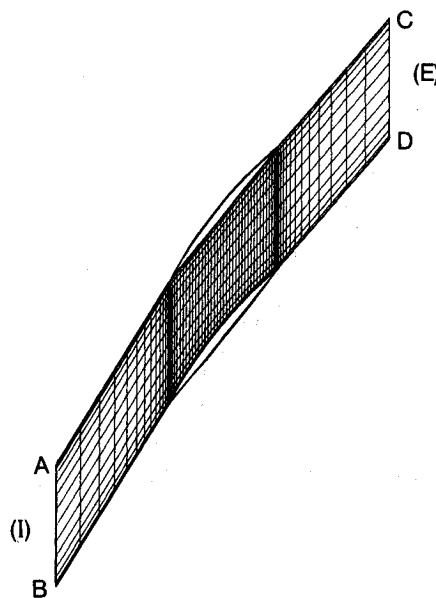


Fig. 8 Two-dimensional supersonic inlet cascade grid, 9.5% DCA blades, stagger = 51.35 deg, chord/pitch = 1.462, coarse grid used (65×15) , 896 bilinear elements, 41 points on blade; fine grid used (73×25) ; 1728 elements, 49 points on blade. Only coarse grid is shown.

back pressure existing in an isentropic flow and, hence, the exit flow angle is also an unknown. As in the nozzle problem, the shock losses must be calculated to uniquely position the shock.

No potential solution exists today that accounts for all the aforementioned effects simultaneously. For example, Ref. 7 presents solutions of supersonic cascades but does not attempt to determine the unique incidence, while Ref. 8 solutions are carried out past the choking Mach number in order to study the effects of artificial viscosity.

The governing equation for a planar cascade is identical to Eq. (9) and for an annular cascade x is taken to be the

Table 1 Results for staggered cascade with supersonic inlet: unique incidence and choking phenomena; fine grid (73 × 25)

Case	M_I	β_I , deg	\dot{m} lb/s	P_{SB} psia	$\Delta\Phi$
1	1.099	60.10	0.1158	10.91	245
2	1.114	59.04	0.1192	10.82	250
3	1.126	58.28	0.1217	10.63	264
4	1.126	58.28	0.1217	10.52	268
5	1.126	58.28	0.1217	10.44	272

N.B.: Initial values: $M_I = 1.125$; $\beta_I = 58.30$ deg; $q_I \sin \beta_I = 954.5$: fixed.

meridional distance m and y the circumferential distance $rd\theta$

$$(\bar{\rho} \Phi_m)_m + \frac{1}{r} \left(\frac{\bar{\rho}}{r} \Phi_\theta \right)_\theta = 0 \quad (12)$$

and the associated boundary conditions of no-penetration at blade surfaces and periodic flow on grid lines separated by a pitch distance.

We present a numerical approach capable of capturing the physical phenomena just discussed and the procedure is illustrated in Fig. 7 for the cascade of Fig. 8. An initial inlet Mach number (M_I) and flow angle (β_I) are chosen at the inlet (I) of the supersonic cascade to achieve a certain whirl component ($M_I \cdot \sin \beta_I$), which is kept constant during the entire iterative procedure. The distribution of potential $\Phi_I(y)$ at the inlet is thus specified and remains constant. An arbitrary initial value of $\Delta\Phi(\Phi_D - \Phi_B)$, between inlet and exit, is chosen. The exit flow angle (β_E) and, hence, the distribution of Φ on the exit (E), are determined from the exit Mach number (M_E) corresponding to a desired back pressure (p_{SB}). As the solution evolves, M_I and β_I change and the distribution of $\Phi_E(y)$ is recalculated accordingly. Once a residual convergence of $R_{L-2} = 10^{-6}$ is achieved, the inner loop solution is judged to have converged between M_I , β_I , and β_E for a given $\Delta\Phi$. At this stage the numerical static exit pressure (p_{SE}) is checked against the desired back pressure (p_{SB}) and a new value of $\Delta\Phi$ imposed to adjust the back pressure. The outer iterative loop is completed when $p_{SE} = p_{SB}$.

Results are presented in Table 1 with an initial guess of $M_I = 1.125$, $\beta_I = 58.3$ deg. The problem is solved for the range of back pressures shown and the corresponding converged value of $\Delta\Phi$ is determined for each back pressure. The specified back pressure uniquely determines the permissible inlet Mach number and flow angle. As the back pressure is lowered the cascade chokes (Fig. 9) and results of Table 1 confirm the correct behavior of the model in numerically predicting the same incidence angle and inlet Mach number for all choked cases. A similar approach to that of Fig. 7 can also be applied to the general choked cascade case with subsonic inlet Mach numbers.

Figure 10 shows the blade surface Mach number distribution for two back pressures from Table 1 for the fine grid comparison. Figure 11 describes the numerical mass flow rate convergence with iteration at the inlet, a midchannel section, and the exit. It is interesting to note how the mass at inlet and exit start at different ends and converge to the channel mass flow. The choking mass-flow rate emerges naturally with the solution. Similar conclusions have been observed with the flow in the two-dimensional nozzle, and this behavior can be used to accelerate iteration convergence.

Stream Function Formulation

If we introduce a stream function Ψ such that

$$\bar{\rho}u = \Psi_y; \quad \bar{\rho}v = -\Psi_x \quad (13)$$

mass is automatically conserved. The governing equation for Ψ , with artificial compressibility, is

Fig. 9 Choked flow in supersonic cascade of Fig. 8, (73 × 25) grid.

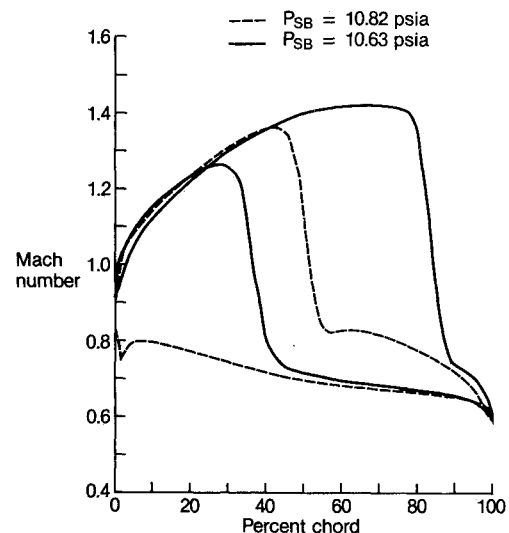
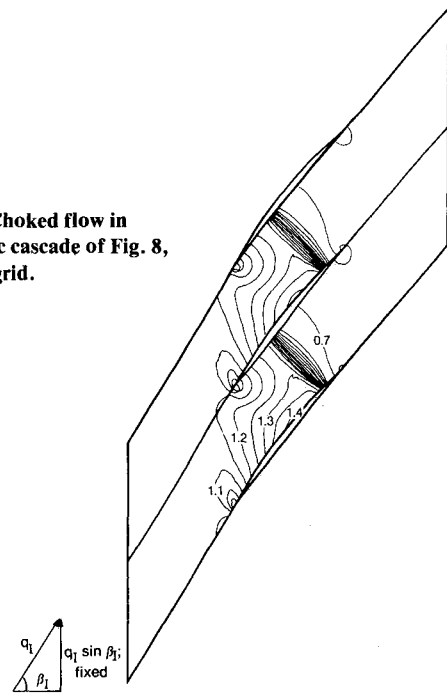


Fig. 10 Surface Mach number distribution for supersonic cascade for back pressures 2 and 3 of Table 1, (73 × 25) grid.

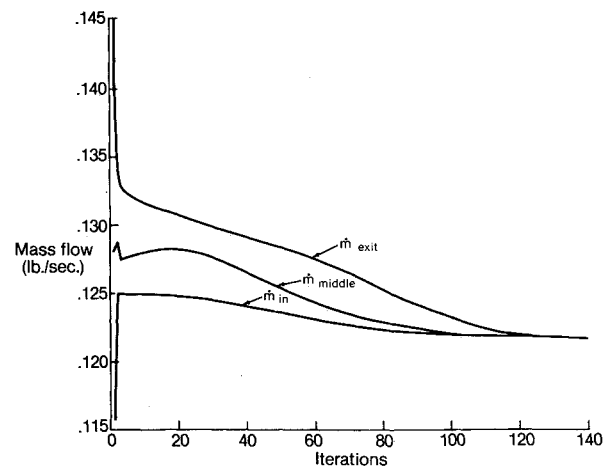


Fig. 11 Convergence of numerical mass flow with iteration at inlet, midchannel, and exit of cascade of Fig. 8.

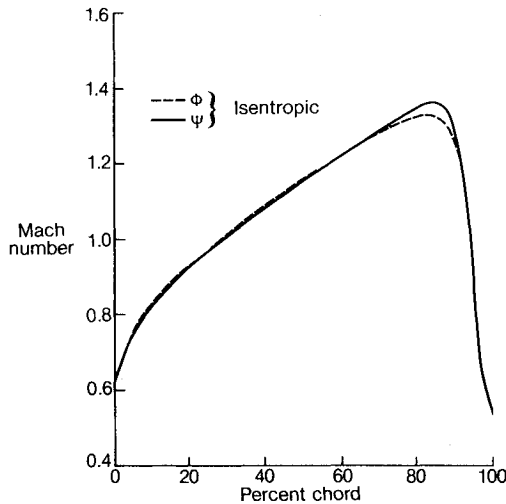


Fig. 12 Results of stream function and classical potential isentropic solutions for flow in a two-dimensional nozzle formed by 4.2% circular arc bump, height/chord = 2, $M_I = 0.8385$.

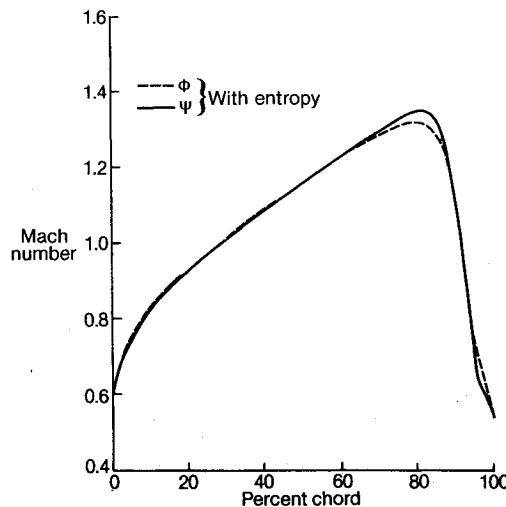


Fig. 13 Results of stream function and modified potential nonisentropic irrotational solutions for flow over 4.2% circular bump.

$$\left(\frac{\Psi_x}{\bar{\rho}}\right)_x + \left(\frac{\Psi_y}{\bar{\rho}}\right)_y = -\omega \quad (14)$$

The associated boundary conditions are

$$\Psi = \text{const on walls} \quad (15a)$$

$$\Psi_x = 0 \text{ at inlet and exit} \quad (15b)$$

with a ceiling on the Ψ value on the outer wall corresponding to the choking condition.

The vorticity ω is calculated through Crocco's relation

$$\frac{\omega}{\bar{\rho}} = \frac{d(\Delta S/\bar{R})}{d\Psi} \quad (16)$$

Hence, the vorticity can be calculated at each grid point downstream of the shock once the stream function distribution is known. If both entropy generation and vorticity are neglected, the stream function and potential formulations are equivalent. If only the entropy is retained, the formulation is equivalent to the modified potential described previously. With both entropy and vorticity activated the stream function results should agree with the Euler solution.

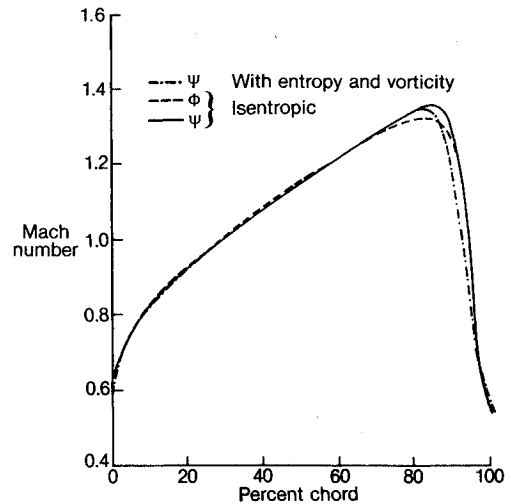


Fig. 14 Results of stream function nonisentropic, rotational solution for flow over 4.2% circular bump, and comparison to isentropic solutions.

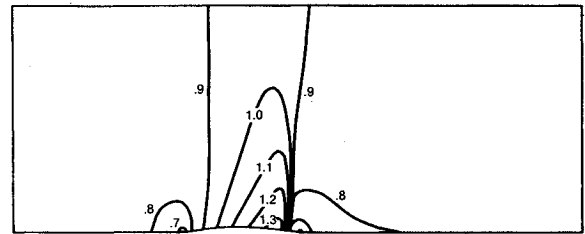


Fig. 15 Mach number contours for flow of Fig. 14.

Numerical results for a nozzle formed by a 4.2% circular arc bump (similar to Ref. 9) are presented in Figs. 12-14.

In Figs. 12 and 13 the potential solutions, with and without entropy correction, are shown for comparison and, except for the peak Mach number, match the corresponding stream function solutions well. Figure 15 presents the Mach number contours for the nonisentropic stream function solution shown in Fig. 14, with vorticity. The details of the calculation concerning discretization, formulation, and solution of the equations are the same as in Ref. 10.

Concluding Remarks

Numerical simulations of internal flows, including nonisentropic effects, are presented using both a modified potential and a stream function formulation. For choked flows the inclusion of nonisentropic effects is essential to obtain a solution as demonstrated by the nozzle problem. In addition, a numerical solution of supersonic cascades with unique incidence is presented for the first time using a potential formulation. Vorticity effects are not critical in many cases but they can be easily accounted for in the stream function formulation, if needed.

Acknowledgments

The authors would like to thank the engineering staff of Pratt & Whitney Canada for their assistance with some of the calculations. This research was supported by Contract PRAI-P-8219 and Grant A-3662 of the Natural Sciences and Engineering Council of Canada (NSERC) and by Pratt & Whitney Canada Inc.

References

- 1 Hafez, M. M., South, J., and Murman, E., "Artificial Compressibility Methods for Numerical Solutions of Transonic Full Potential Equation," *AIAA Journal*, Vol. 17, Aug. 1979, pp. 838-844.

²Habashi, W. G. and Hafez, M. M., "Finite Element Solutions of Transonic Flow Problems," *AIAA Journal*, Vol. 20, Oct. 1982, pp. 1368-1376.

³Deconinck, H. and Hirsch, Ch., "Boundary Conditions for the Potential Equation in Transonic Internal Flow Calculations," ASME Paper 83-GT-135.

⁴Hafez, M. M., "Progress in Finite Element Techniques for Transonic Flows," AIAA Paper 83-1919, *Proceedings, AIAA 6th Computational Fluid Dynamics Conference*, July 1983, pp. 243-250.

⁵Kantrowitz, A., "The Supersonic Axial Flow Compressor," NACA Rept. 974, 1950.

⁶Erwin, J. R. and Ferri, A., "The Supersonic Compressor," *Aerodynamics of Turbines and Compressors*, edited by W. R. Hawthorne, Princeton University Press, 1964, pp. 368-432.

⁷Hirsch, C. and Deconinck, H., "A Survey of Finite Element Methods for Transonic Flows," *Numerical Methods in Aeronautical Fluid Dynamics*, edited by P. L. Roe, Academic Press, 1982, pp. 143-188.

⁸Akay, H. U. and Ecer, A., "Finite Element Analysis of Transonic Flows in Highly Staggered Cascades," *AIAA Journal*, Vol. 20, March 1982, pp. 410-416.

⁹Notes on Numerical Fluid Mechanics, *GAMM Workshop on Numerical Methods for the Computation of Inviscid Transonic Flows with Shock Waves*, edited by A. Rizzi and H. Viviand, Vieweg & Sohn, 1980.

¹⁰Habashi, W. G. and Hafez, M. M., "Finite Element Stream Function Solutions for Transonic Turbomachinery Flows," AIAA Paper 82-1268, June 1982.

From the AIAA Progress in Astronautics and Aeronautics Series . . .

VISCOUS FLOW DRAG REDUCTION—v. 72

Edited by Gary R. Hough, Vought Advanced Technology Center

One of the most important goals of modern fluid dynamics is the achievement of high speed flight with the least possible expenditure of fuel. Under today's conditions of high fuel costs, the emphasis on energy conservation and on fuel economy has become especially important in civil air transportation. An important path toward these goals lies in the direction of drag reduction, the theme of this book. Historically, the reduction of drag has been achieved by means of better understanding and better control of the boundary layer, including the separation region and the wake of the body. In recent years it has become apparent that, together with the fluid-mechanical approach, it is important to understand the physics of fluids at the smallest dimensions, in fact, at the molecular level. More and more, physicists are joining with fluid dynamicists in the quest for understanding of such phenomena as the origins of turbulence and the nature of fluid-surface interaction. In the field of underwater motion, this has led to extensive study of the role of high molecular weight additives in reducing skin friction and in controlling boundary layer transition, with beneficial effects on the drag of submerged bodies. This entire range of topics is covered by the papers in this volume, offering the aerodynamicist and the hydrodynamicist new basic knowledge of the phenomena to be mastered in order to reduce the drag of a vehicle.

456 pp., 6 × 9, illus., \$25.00 Mem., \$40.00 List

TO ORDER WRITE: Publications Order Dept., AIAA, 1633 Broadway, New York, N.Y. 10019